GEOPHYSICAL RESEARCH LETTERS, VOL. 24, NO. 22, PAGES 2913-2916, NOVEMBER 15, 1997

Non-Maxwellian particle distributions and electromagnetic ion cyclotron instabilities in the near-Earth magnetotail

C. C. Chaston[1], Y. D. Hu and B. J. Fraser
Department of Physics, University of Newcastle, New South Wales, Australia

Abstract. Ion distributions in the near-Earth magnetotail often deviate significantly from a bi-Maxwellian, the form usually assumed in previous studies of instability in this region of space. Here the electromagnetic dispersion equation for propagation parallel to the background magnetic field is derived from the linearised Vlasov equation for both the generalised bi-Lorenztian (kappa) distribution and a crescent shaped distribution. For the hot drifting proton distributions in the near Earth magnetotail it is found that increasing deviation from bi-Maxwellian toward bi-Lorentzian and crescent shaped forms reduces the maximum temporal growth rates and extends the range of wavenumbers and frequencies where instability occurs. The extension of the range of unstable wavenumbers has the significant effect of increasing convective growth rates in the vicinity of the crossover frequency.

Introduction

Studies of the differential energy spectra of particles in the plasma sheet and plasma sheet boundary layer [De Coster and Frank, 1979; Christon et al., 1991] indicate that velocity distributions in the near-earth magnetotail exhibit Maxwellian functional form below the thermal energy, and extended high-energy tails having power law form above the thermal energy. These distributions most closely fit bi-Lorentzian or kappa profiles [Vasyliunas, 1971; Summers and Thorne, 1992] over the entire energy range. Further, the proton beam components characteristic of the plasma sheet boundary layer typically exhibit a characteristically crescent-like shape [DeCoster and Frank, 1979; Nakamura et al., 1992]. The presence of both a high energy proton tail and a cresent shaped hot proton beam may have significant effects upon electromagnetic instabilities driven by the proton temperature anisotropy and the relative drift between components in the plasma.

Xue et al. [1993, 1996a,b] have investigated the influence of enhanced resonant high energy ion tail populations on field-aligned instability characteristics using bi-Lorentzian distributions. In this paper we investigate the significance of these effects and the importance of crescent shaped proton beams for the streaming particle distributions characteristic of the near-Earth plasma sheet boundary layer. First the dispersion equations derived from linear Vlasov theory for drifting bi-Lorentzian distributions and crescent-shaped beams are presented. Then the numerical solutions of these equations for parameters typical of the near-Earth magnetotail are presented. Finally the implications of the results for electromagnetic wave growth and dispersion in the near Earth magnetotail are discussed.

Dispersion Relations

The dispersion relation for electromagnetic waves propagating along the magnetic field in a homogeneous magnetised [Gary, 1993] plasma can be expressed as,

$$D^{\pm}(k_{\|},\omega) = \omega^2 - k_{\|}^2c^2 + k_{\|}^2c^2\sum_j S_j^{\pm}(k_{\|},\omega) \quad (1)$$

where $S_j^{\pm}$ is the plasma conductivity tensor determined by the form of the particle distribution function for the jth component. From Summers and Thorne [1992] the bi-Lorentzian distribution for the jth component in a plasma with drift v_{0j} along the field has the form,

$$F_j(v_{\|},v_{\perp}) = \frac{N_{\kappa j}}{\left[1+\frac{(v_{\|}-v_{0j})^2}{\kappa_j v_{\|\kappa_j}}+\frac{v_{\perp}^2}{\kappa_j v_{\perp\kappa_j}}\right]^{\kappa_j+1}} \quad (2)$$

where $N_{\kappa j}$ is a normalization constant required to ensure $\int F_j d^3v = 1$ and $v_{\|\kappa j}$ and $v_{\perp\kappa j}$ are the thermal velocities parallel and perpendicular to the background magnetic field. $N_{\kappa j}$, $v_{\|\kappa j}$ and $v_{\perp\kappa j}$ are identical to those given by Summers and Thorne (1992).

Solving the linearized Vlasov equation in the traditional manner [Gary, 1993] yields the conductivity tensor for parallel propagating electromagnetic waves in a bi-Lorentzian plasma,

$$S_{\kappa_j}^{\pm}(v_{\|},v_{\perp}) = \frac{\omega_j^2}{k_{\|}^2c^2}\left[\frac{\omega-k_{\|}v_{0j}}{k_{\|}v_{\|\kappa_j}}\left(\frac{\kappa_j}{\kappa_j-3/2}\right)\left(\frac{\kappa_j-1}{\kappa_j}\right)^{3/2}\right.$$
$$\times Z_{\kappa_j-1}\left(\sqrt{\frac{\kappa_j-1}{\kappa_j}}\xi_j^{\pm}\right)-\left(1-\frac{T_{\perp j}}{T_{\|j}}\right)$$
$$\left.\times\left(1+\left(\frac{\kappa_j-1_j}{\kappa_j-3/2}\right)\sqrt{\frac{\kappa_j-1}{\kappa_j}}\xi_j^{\pm}Z_{\kappa_j-1}\left(\sqrt{\frac{\kappa_j-1}{\kappa_j}}\right)\right)\right] \quad (3)$$

where $\xi_j^{\pm} = (\omega - k_{\|}v_{0j} \pm \Omega_j)/(k_{\|}v_{\kappa j})$ and $Z_{\kappa j-1}$ is the modified plasma dispersion function for the generalised Lorentzian distribution suggested by Summers and Thorne [1991].

To model the crescent shaped proton beam distributions of the plasma sheet boundary layer and maintain the convenience of separability in $v_{\|}$ and $v_{\perp}$ we generalize the distribution function presented by Gary and Sinha [1989] to yield

$$F_s(v_{\|},v_{\perp}) = C_n\left(\frac{(av_{\perp})^2+(bv_{\|})^2}{v_s^2}\right)^n\cdot\frac{n_s}{(2\pi v_s^2)^{3/2}}$$
$$\times\exp\left(\frac{-(v_{\perp}^2+v_{\|}^2)}{v_s^2}\right) \quad (4)$$

[1]Now at Space Sciences Laboratory, University of California at Berkeley

Paper number 97GL02972.
0094-8534/97/97GL-02972$05.00

where $v_s=(2T_s/m_s)^{1/2}$, n_s is the shell number density, n is a fitting parameter determined by the curvature and temperature of the distribution and C_n is a normalization constant given by,

$$C_1 = 1/(2a^2+b^2)$$
$$C_2 = 1/(8a^4+4a^2b^2+3b^4)$$
$$C_3 = 1/(48a^6+24a^4b^6+6a^2b^4+5b^6) \quad (5)$$

If a=b=1 this distribution describes a full shell as studied by Gary and Sinha [1989]. If a<b then this distribution describes a partial shell resembling two crescent shaped beams symmetrical about v=0 Conversely, if a>b then this distribution resembles a ring beam often observed in cometary plasmas [Balsiger et al., 1986]. Figure 1 illustrates the form of this distribution for a=0.6, b=1 and n=2. Of note in this figure is the sharp low energy cutoff along $v_{||}$ for each beam which is consistent with observations [Eastman et al., 1986, Kawano et al., 1994].

Solving the linearised Vlasov equation for this distribution with n=2 yields the conductivity tensor,

$$S_s^{\pm}(\omega,k_{||}) = \frac{-2\omega j}{k_{||}^2c^2}.C_n\left[\frac{\omega}{v_s k_{||}}\left(\frac{-b^4}{2}(\xi_s^{\pm 2}Z'(\xi_s^{\pm})-\xi_s^{\pm}Z(\xi_s^{\pm})) + 2a^2b^2\xi_s^{\pm}Z(\xi_s^{\pm}) - 4a^4Z(\xi_s^{\pm})\right) - 2a^2b^2 + 2b^4 + Z(\xi_s^{\pm})\left((2a^2b^2-2b^4)\xi_s^{\pm 2} - 2a^4 - 4a^2b^2 + 6b^4\right)\right] \quad (6)$$

where Z is the plasma dispersion function as defined by Fried and Conte [1961].

Numerical results

The plasma model used to represent the multi-component particle distributions of the plasma sheet is given in Table 1 and follows from the observations of Eastman et al. [1986], Angelopoulos et al. [1989], and Chaston et al. [1994]. Solutions of the Equation (1) for these moments using the conductivity tensor of Equation (3) with $\kappa=\infty$ indicates that thermal effects and the Doppler shift act to remove stop bands and allow growth and wave propagation almost continuously through the He^+ and O^+ resonances. As a result the growing wave dispersion characteristics vary little from that of the two species proton-electron plasma studied by Angelopoulos et al. [1989] and Chaston et al. [1994].

Bi-Lorentzian Ditstributions

Previous studies of magnetospheric plasmas [Summers and Thorne, 1992; Xue et al., 1993] have shown that the increase in density of high energy particles in the extended tail of the Lorentzian distribution can enhance electromagnetic wave growth rates relative to those in a Maxwellian plasma. However as indicated by Xue et. al. [1996b] for ion cyclotron instabilities this enhancement is particularly sensitive to anisotropy and plasma β of the unstable proton component. For distributions typical of the equatorial magnetosphere with high values of β(≈1) Xue et al. [1996b] finds that as κ of the hot anisotropic proton component is decreased (thereby increasing the plasma density in the energetic tail) maximum growth rates fall in response to the decrease in $\partial F/\partial v$ at the resonant velocity. In the same way, for the parameters prevailing in the near-Earth magnetotail, decreasing the κ index of the anisotropic proton beam component decreases the maximum growth rate of the ion cyclotron anisotropy instability. This effect is made apparent in Figure 2 which presents the solutions to Equation (1) for the parameters of Table (1) with several values of κ from ∞ to 2. Over this range of κ values, γ_{max}/Ω_p falls from 0.092 to 0.059. The instability does, however, extend over a broader frequency range as κ is decreased since the instability extends to lower wavenumbers consistent with the results of Xue et al. [1993].

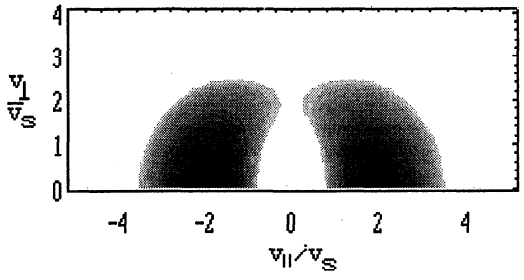

Figure 1. Normalised density plot of $\log_{10}F_s(v_{||},v_\perp)$ given by Equation (4) for n=2, a=0.6, and b=1.

Table 1. Normalised plasma parameters for the near-Earth plasma sheet boundary layer. Core and beams are protons.

Component	$T_{\perp j}/T_{\perp c}$	$T_{\perp j}/T_{||j}$	v_{0j}/v_A	n_j/n_t
Core	1.0	1.0	0.0	0.192
Parallel Beam	50.0	8.0	0.6	0.384
Anti-parallel Beam	50.0	8.0	-1.0	0.064
He^+	1.0	1.0	0.0	0.030
He^{++}	10.0	1.0	0.0	0.030
O^+	1.0	1.0	0.0	0.300
Electrons	1.0	1.0	0.0	1.030

Here $\beta_{\perp c}=0.01$ and $v_A/c=0.005$ where $\beta_{\perp c}=8\pi n_t/B_0^2$ and $v_A=B_0/(4\pi n_t m_p)^{1/2}$.

The extension in the range of unstable wavenumbers with decreasing κ significantly alters convective growth rates from the bi-Maxwellian case. Figure 3 illustrates the convective growth rate curves for κ=∞, 10, 6, 4, 3, 2 calculated from the real frequency and growth rate curves of Figure 2. These curves have similar form to those calculated by Horne and Thorne (1994) and Xue et al. (1996a,1996b) where peaks correspond to those wavenumbers where $\partial\omega/\partial k\rightarrow 0$. However, the lack of stopbands and the effects of doppler shifts in magnetotail plasmas provide significantly different group velocities over unstable wavenumbers from that in dayside equatorial plasmas so that the character of convective wave growth here is considerably modified from the dayside case.

From Figure 3 it is clear that at lower wavenumbers the bi-Lorentzian distribution provides convective growth rates several orders of magnitude greater than the bi-Maxwellian

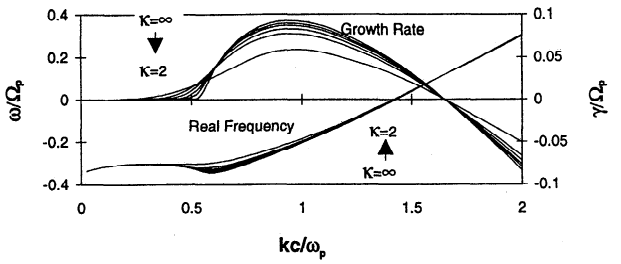

Figure 2. Dispersion curves from the solution of Equation (1) using the conductivity tensor of Equation (3) and the parameters of Table 1 with a parallel proton beam where κ=∞, 10, 6, 4, 3, and 2. For simplicity only those real frequency curves which have positive imaginary components are plotted.

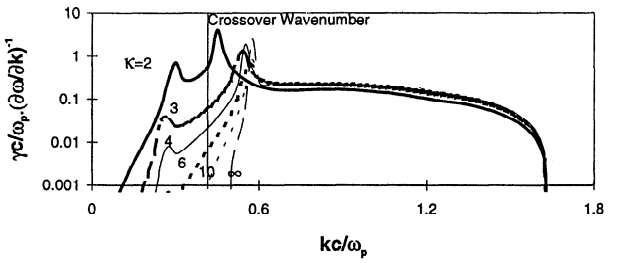

Figure 3. Convective growth rates for $\kappa=\infty$, 10, 6, 4, 3, and 2 calculated from the results illustrated in Figure 3. The crossover wavenumber is the wavenumber corresponding to the crossover frequency.

distribution. With decreasing κ the wave group velocity is significantly reduced relative to the corresponding bi-Maxwellian result at wavenumbers mapping to frequencies in the vicinity of the crossover frequency. For κ=4,3,2 an additional hump in convective growth rate occurs which is indicative of the extension of instability to wavenumbers which map to frequencies just above the ion hybrid frequency between Ω_{He}^{+} and Ω_{He}^{++}, and below the crossover frequency. The contribution of this additional peak to observed wave spectra however should be small since waves in this range are unguided (Horne and Thorne, 1994) and may rapidly convect out of the field-aligned source region before growing to significant amplitudes. From the normalisation employed a total ion density of 0.1 cm^{-3} yields an e-folding distance of 720 km at $\gamma c/\omega_p.(\partial\omega/\partial k)^{-1}=1$. Consequently, the spatial size for growth to observable levels, based on 10 e-foldings (Horne and Thorne, 1994), is of the order of 1 Re for the most slowly travelling wave frequencies corresponding to the largest convective growth rate, and a few Re at those wavenumbers where maximum temporal growth occurs.

Crescent Shaped Beam Distributions

Table 2 contains the parameters employed in examining the effects of decreasing beam curvature upon wave dispersion and growth where the value of 'a' in Equation (6) is varied from 1 to zero with 'b' held fixed at unity. The solutions of Equation (1) for the parameters of Table 2 are presented in Figure 4. Since proton distributions approaching a full shell occur closer to the plasma sheet, $\beta_{\perp c}$ is in this case larger than for the distribution in Table 1 reflecting increased plasma density and core temperature with proximity to the plasma sheet. For an n=2 shell these parameters result in a shell radius greater than the Alfven speed and consequently the dominant instability arising during the transition from full to partial shells will be the right-hand resonant instability. To realistically examine the effects of beam curvature upon ion cyclotron anisotropy instability higher values of n must be employed to provide the requisite anisotropy. Derivation of $S_s^{\pm}$ however becomes increasingly tedious with increasing values of n and has not been attempted here.

Table 2. Normalised plasma parameters substituted into Equation (1) to obtain the dispersion curves of Figure 4.

Comp	$T_{\perp j}/T_{\perp c}$	$T_{\perp j}/T_{\parallel j}$	v_{0j}/v_A	n_j/n_e	(a,b)
Core	1	1	0	0.4	-
Shell	30	1	0	0.6	(1,0), (0.8,1), (0.6,1), (0.4,1), (0.2,1), (0,1)
Elec-	1	1	0	1	-

Here $\beta_{\perp c}$=0.1 and v_A/c=0.0015.

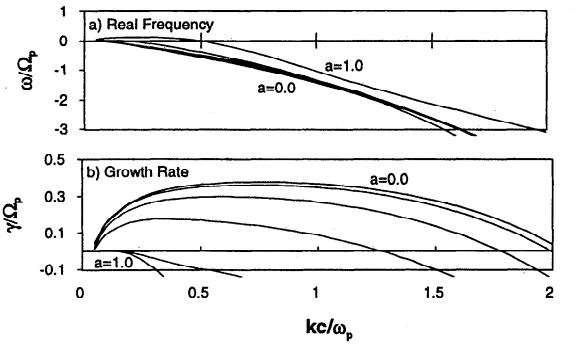

Figure 4. Dispersion curves from the solution of Equation (1) using the conductivity tensor of Equation (6) and the parameters of Table 2 for a=1.0, 0.8, 0.6, 0.4, 0.2, 0.0 and b=1.0 . (a) contains real frequencies while (b) contains growth rates.

When a=b=1 the dispersion curves given in Figure 4(a) indicate that the Alfven wave branch is strongly Doppler shifted becoming right-hand polarized when kc/ω_p >0.5 and is stable, in agreement with the full shell results of Gary and Sinha (1989) and Freund and Wu (1988), When a=0.8 the resulting partial shell distribution can be considered as two symmetrical beams about $v_{\parallel}$=0 so that the effective density of ions with significant parallel drift is enhanced. As a consequence, the Alfven branch experiences an increased Doppler shift and becomes almost exclusively right-hand polarized except for when kc/ω_p<0.25 where Figure 4(b) indicates that the anisotropy instability provides small growth for left-hand polarised waves. As 'a' decreases towards zero the anisotropy and curvature of the beam components decreases whilst the effective beam velocity increases. This effect is clearly expressed by the increasing growth rate of the right-hand resonant instability with decreasing 'a'. At a=0 the dispersion results return exactly to those expected for a pair of bi-Maxwellian beams symmetric about $v_{\parallel}$=0.

To evaluate the significance of beam curvature we generated a phase space density grid of $F_s(v_{\parallel}, v_{\perp})$ for both a=0.6 and a=0.2 and the temperatures and densities given in Table 2. Moment integrations over these grids are then performed to provide temperatures and drift velocities as would be performed over an observed beam distribution under the assumption that the observed beam held bi-Maxwellian form. The parameters for the partial shell and the moment results for the 'bi-Maxwellian' beams are presented in Table 3 and the dispersion results obtained for each are compared in Figure 5. Figure 5(a) shows that for a=0.6 both the partial shell and bi-Maxwellian beam

Table 3. Equivalent bi-Maxwellian parameters for two partial shell distributions where n_s/n_e=0.6, $T_s/T_{\perp c}$=30 and n=2. Core and shell proton and electron parameters for modelling are taken from Table 2.

Partial Shell	Parameter	Parallel Beam	Anti-parallel Beam
a=0.6, b=1	v_{0j}/v_A	2.15	-2.15
	$T_{\perp j}/T_{\perp c}$	25	25
	$T_{\perp j}/T_{\parallel j}$	2.35	2.35
	n_j/n_e	0.3	0.3
a=0.2, b=1	v_{0j}/v_A	2.57	-2.57
	$T_{\perp j}/T_{\perp c}$	15.9	15.9
	$T_{\perp j}/T_{\parallel j}$	2.15	2.15
	n_j/n_e	0.3	0.3

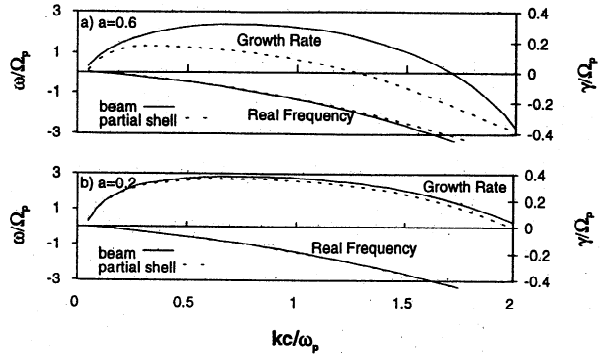

Figure 5. Comparison of the dispersion properties of crescent shaped or partial shell distributions (dashed curves) with equivalent bi-Maxwellian beam distributions (solid curves) for a=0.6, 0.2, n=2, b=1 and the plasma parameters given in Table 3.

parameters provide growth for the right-hand resonant instability. However, the bi-Maxwellian beam parameters provide larger growth over a larger range of wavenumbers since the density is distributed more closely to v_{max} ($v_{||}$ where $F_j(v_{||}, v_\perp)$ is largest) and $-v_{max}$, than for the partial shell case where the ion distribution extends almost continuously from v_{max} to $-v_{max}$. This effectively decreases the relative drift between beam and core components and the population of resonant ions, hence the lower growth rate. When a=0.2 (Figure 5(b)) almost identical results for the bi-Maxwellian beam and partial shell distribution are obtained.

Discussion and Conclusions

The deviation from bi-Maxwellian towards bi-Lorentzian form has significant implications for wave growth and dispersion when $\kappa \leq 4$. While decreasing κ reduces temporal growth rates and frequencies, it significantly enhances convective growth rates in the vicinity of the crossover frequency and the ion hybrid frequency between the He^+ and He^{++} resonances. The enhancement results from the reduction of the wave group velocity for both guided and unguided waves on either side of the wavenumber corresponding to the crossover frequency. This indicates that Lorentzian distributions require smaller source regions (of the order of 1 Re) for growth to observable levels in the magnetotail and may allow growth to larger amplitudes particularly at at wavenumbers which map close to the crossover frequency. Comparison of Figure 3 and Figure 2 indicates that the crossover frequency (for parameters based on those of Chaston et al., 1994) occurs at ~0.3 Ω_p. This frequency falls close to peak in polarised wave power reported by Chaston et al. (1994) and within the frequency range of the more broadbanded observations reported by Angelopoulos et al. (1989).

Furthermore, this study has introduced a modified Maxwellian distribution function which accurately represents the crescent-like shape of proton beams in the plasma sheet boundary layer. Solution of the linear Vlasov equation for this distribution indicates that beam curvature or a crescent-like shape reduces the wave temporal growth rate for resonant instabilities relative to the equivalent bi-Maxwellian result but with little effect upon wave dispersion. This is an expected result since increasing beam curvature reduces the anisotropy, relative drift between components and the population of strongly resonant ions. These results emphasize the importance of providing an accurate representation of the particle distribution function for the modelling of observed wave spectra resulting from electromagnetic microinstabilities.

Acknowledgments. The authors would like to acknowledge the useful suggestions of S. P. Gary in the preparation of this manuscript. This research was supported by grants from the Australian Research Council, the University of Newcastle and NSF grant ATM9224688.

References

Angelopoulous, V., R. C. Elphic, S. P. Gary, and C. Y. Huang, Electromagnetic instabilities in the plasma sheet boundary layer, *J. Geophys. Res., 94*, 15373, 1989.

Balsiger, H., K. Altwegg, F. Buhler, J. Geiss, A. G. Ghielmetti, B. E. Goldstein, W. T. Huntress, W. H. Ip, A. J. Lazarus, A. Meier, M. Neugebauer, U. Rottenmund, H. Rosenbauer, R. Schwenn, R. D. Sharp, E. G. Shelley, E. Ungstrup, and D. T. Young, Ion composition and dynamics at comet Halley, *Nature, 321*, 330, 1986.

Chaston, C. C., Y. D. Hu, B. J. Fraser, R. C. Elphic, and C. Y. Huang, Electromagnetic ion cyclotron waves observed in the near earth plasma sheet boundary layer, *J. Geomag. Geoelectr., 46*, 987, 1994.

Christon, S. P., D. J. Williams, D. G. Mitchell, C. Y. Huang, and L. A. Frank, Spectral characteristics of plasma sheet ion and electron populations during disturbed geomagnetic conditions, *J. Geophys. Res., 96*, 1, 1991.

DeCoster, R. J., and L. A. Frank, Observations pertaining to the dynamics of the plasma sheet, *J. Geophys. Res., 84*, 5099, 1979.

Eastman, T. E., R. J. De Coster, and L. A. Frank, Velocity distributions of ion beams in the plasma sheet boundary layer, in *Ion Acceleration in the magnetosphere and ionosphere, Geophys. Monogr. Ser.*, vol 38, edited by T. Chang, p 117-126, AGU, Washington D. C., 1986.

Freund H. P., and C. S. Wu, Stability of a spherical shell distribution of pickup ions, *J. Geophys. Res.,93*, 14277, 1988.

Fried, B. D., and S. D. Conte, The plasma dispersion function, Academic Press, San Diego, 1961.

Gary, S. P., and R. Sinha, Electromagnetic waves and instabilities from cometary ion velocity shell distributions, *J. Geophys. Res., 94*, 9131, 1989.

Gary, S. P., *Theory of space plasma microinstabilities*, Cambridge Atmospheric and Space Science Series, Cambridge University Press, Cambridge, 1993.

Horne, R. B., and, R. M. Thorne, Convective instabilities of electromagnetic ion cyclotron waves in the outer magnetosphere, *J. Geophys. Res., 99*, 17259, 1994.

Kawano, H., M. Fujito, T. Mukai, T. Yamamoto, T. Terasawa, Y. Saito, S. Machida, S. Kokubun, and A. Nishida, Right-handed ion/ion resonant instability in the plasma sheet boundary layer: GEOTAIL observation in the distant tail, *Geophys. Res. Lett., 25*, 2887, 1994.

Nakamura M. , G. Paschmann, W. Baumjohann, and N. Sckopke, Ion distributions and flows in and near the plasma sheet boundary layer, *J. Geophys. Res., 97*, 1449, 1992.

Summers, D., and R. M. Thorne, The modified plasma dispersion function, *Phys. Fluids B, 3*, 1835, 1991.

Summers, D., and R. M. Thorne, A new tool for analyzing microinstabilities in space plasmas modeled by a generalised Lorentzian (Kappa) distribution, *J. Geophys. Res., 97*, 16827, 1992

Vasyliunas, V., Deep space plasma measurements, in *Methods of experimental physics: Plasma Physics, Part B*, vol. 9, edited by R. H. Lovberg and H. R. Griem, p 49-88, Academic, Orlando, Fla., 1971.

Xue, S., R. M. Thorne and D. Summers, Electromagnetic ion-cyclotron instability in space plasmas, *J. Geophys. Res., 98*, 17475, 1993.

Xue, S., R. M. Thorne and D. Summers, Growth and damping of oblique electromagnetic ion cyclotron waves in the Earth's magnetosphere, *J. Geophys. Res., 101*, 15457, 1996a.

Xue, S., R. M. Thorne and D. Summers, Parametric study of electromagnetic ion cyclotron instability in the Earth's magnetosphere, *J. Geophys. Res., 101*, 15467, 1996b.

C. C. Chaston, Space Sciences Laboratory, University of California, Berkeley, CA94720-7450 (e-mail: ccc@ssl.berkeley.edu).

B. J. Fraser and Y.D. Hu, Department of Physics, University of Newcastle, Newcastle, NSW 2308, Australia.

(Received July 14, 1997; revised September 26, 1997; accepted October 14, 1997.)